P H Y S I C A L R E V I E W L E T T E R S

Experimental Preparation of Quadripartite Cluster and Greenberger-Horne-Zeilinger Entangled States for Continuous Variables

Xiaolong Su, Aihong Tan, Xiaojun Jia,* Jing Zhang, Changde Xie, and Kunchi Peng

The State Key Laboratory of Quantum Optics and Quantum Optics Devices, Institute of Opto-Electronics, Shanxi University, Taiyuan, 030006, People's Republic of China

The cluster states and Greenberger-Horne-Zeilinger (GHZ) states are two different types of multipartite quantum entangled states. We present the first experimental results generating continuous variable quadripartite cluster and GHZ entangled states of electromagnetic fields. Utilizing two amplitude-quadrature and two phase-quadrature squeezed states of light and linearly optical transformations, the two types of entangled states for amplitude and phase quadratures of light are experimentally produced. The combinations of the measured quadrature variances prove the full inseparability of the generated four subsystems. The presented experimental schemes show that the multipartite entanglement of continuous variables can be deterministically generated with the relatively simple implementation.

In recent years the investigation of a continuous variable (CV) quantum communication network (QCN) has attracted extensive interest along with the development of the experimental performances of quantum information based on CV tripartite Greenberger-Horne-Zeilinger (GHZ) entanglement [1–3]. A variety of complicated CV QCNs exploiting multipartite GHZ entangled states of more than three subsystems have been theoretically proposed [4–7]. In addition, another type of CV multipartite entangled states, CV cluster states, have been theoretically introduced [8]. Successively, Menicucci *et al.* prove that the universal quantum computation (QC) can be achieved with CV cluster states as long as a non-Gaussian measurement can be performed [9]. In the study of quantum information for discrete variables, the five-photon GHZ states [10] and four-photon cluster states [11] have been experimentally demonstrated and successfully applied in open-destination teleportation and one-way quantum computing, respectively. However, the realization of CV cluster and quadripartite GHZ states still remain an experimental challenge. The CV quantum resources, such as squeezed and entangled states of light, emerge from the nonlinear optical interaction of a laser with a crystal in an unconditional fashion. The unconditionalness of the CV implementations makes the CV approach to be particularly suited for further experimental demonstration of the general principles of GHZ-state QCN and cluster-state QC.

In this Letter, we present the experimental schemes to produce CV quadripartite entangled cluster state and GHZ state. Using a pair of nondegenerate optical parametric amplifier (NOPA) we obtained two amplitude-quadrature squeezed states and two phase-quadrature squeezed states, simultaneously. Then, only by means of linearly optical transformation of these squeezed lights under certain phase relations, the CV quadripartite cluster state and GHZ state of electromagnetic field are generated from the system, respectively. The results measured with the balanced-homodyne detectors to the variances of amplitude and phase quadratures demonstrated that the combinations containing both conjugate variables of all four modes satisfy the criteria of the full inseparability of multimodes [12].

It has been theoretically and experimentally demonstrated that the two coupled modes of the original signal and idler modes with orthogonal polarizations from a NOPA are the phase-quadrature and the amplitude-quadrature squeezed states of light, respectively [13–15]. For a NOPA operating at deamplification (the pump light and the injected signal light are out of phase), the superposed mode at $+45°$ polarizing direction is the amplitude-quadrature squeezed state and that at $-45°$ is the phase-quadrature squeezed state [13,16]. The schematic of the experimental system is shown in Fig. 1. The pump laser (Nd:YAP/KTP) is a homemade cw intracavity frequency-doubled and frequency-stabilized Nd-doped $YAlO_3$ perovskite laser with a frequency-doubling crystal KTP (potassium titanyl phosphate) inside the cavity. The second harmonic wave output at 540 nm and the fundamental wave output at 1080 nm from the laser are used for the pump fields and the injected signals of the two NOPAs (NOPA1 and NOPA2), respectively. The two NOPAs were constructed in identical configuration, both of which consist of an α-cut type-II KTP crystal and a concave mirror. The front face of the KTP was coated to be used as the input coupler and the concave mirror as the output coupler of the squeezed states, which was mounted on a piezo-electric transducer (PZT) for locking actively the cavity length of NOPA on resonance with the injected signal at 1080 nm. Through a parametric down-conversion process of type-II phase match, the quadrature squeezed states of light at 1080 nm were produced. The output optical field from NOPA1 (NOPA2) is split by the polarizing beam splitter PBS_1 (PBS_2) to the amplitude-quadrature squeezed state a_2 (a_3) and the phase-quadrature squeezed state a_1 (a_4) (see the inset of Fig. 1). The half-wave plate P_1 and P_2 are used for orienting the polarizations of the light beams
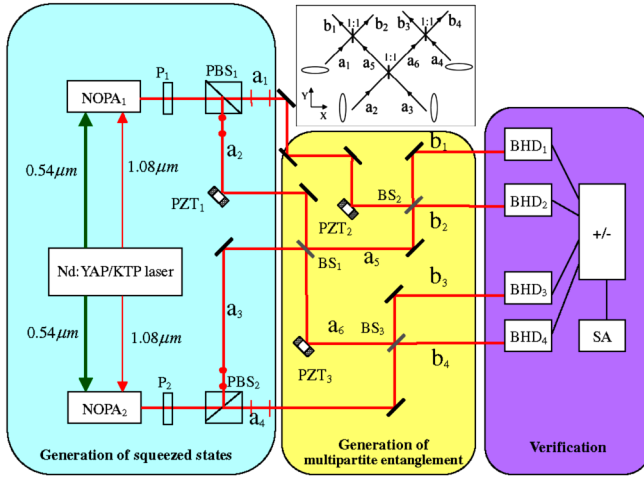
FIG. 1 (color online). Schematic of the experimental setup. Nd:YAP/KTP-laser source; NOPA$_{1-2}$-nondegenerate optical parametric amplifier; P_{1-2}-$\lambda/2$ wave plate; PBS$_{1-2}$-polarizing optical beam splitter; PZT$_{1-3}$-piezoelectric transducer; BS$_{1-3}$-50% optical beam splitter; BHD$_{1-4}$-balanced-homodyne-detectors; $+/-$ -positive/negative power combiner; SA-spectrum analyzer. Inset: a_1, a_4 and a_2, a_3 are phase-quadrature (Y quadrature is squeezed) and amplitude-quadrature (X quadrature is squeezed) squeezed states, respectively. b_1, b_2, b_3, and b_4 combine a quadripartite cluster or GHZ states.

toward PBS$_1$ and PBS$_2$, respectively. The quadrature amplitudes (X_{ai}) and phase (Y_{ai}) of the four squeezed modes a_i ($i = 1, 2, 3, 4$) are expressed by [15,17]

$$X_{a1(4)} = e^{+r}X_{a1(4)}^{(0)}, \qquad Y_{a1(4)} = e^{-r}Y_{a1(4)}^{(0)},$$
$$X_{a2(3)} = e^{-r}X_{a2(3)}^{(0)}, \qquad Y_{a2(3)} = e^{+r}Y_{a2(3)}^{(0)}. \tag{1}$$

Here, r is the squeezing parameter, which depends on the strength and the time of parametric interaction in NOPA, and we have assumed that r for the four squeezed state is identical for simplicity and the requirement is easy to be reached in the experiments if the two NOPAs were constructed in identical configuration and the intracavity losses of the four modes were balanced. The values of r can be from zero to infinite ($r = 0$ no squeezing, $r \rightarrow +\infty$ ideal squeezing and the ideal limit cannot be achieved experimentally since it requires infinite energy). $X_{ai}^{(0)}$ and $Y_{ai}^{(0)}$ stand for the quadrature amplitudes and phases of the injected signal fields into NOPAs. In the calculation we normalized the shot noise limit (SNL) of each submode of quadripartite entangled state to $\frac{1}{4}$ and thus the SNL of total four submodes to 1. In experiments we made all injected quadratures equal. BS$_i$ ($i = 1, 2, 3$) is the 50% beam splitter and PZT$_i$ ($i = 1, 2, 3$) is the piezotransducer. At first interfering modes a_2 and a_3 on BS$_1$ with the phase difference of $\pi/2$ which was controlled by PZT$_1$ and a feedback photoelectronic circuit, we obtained modes a_5 and a_6. Then, combining modes a_1 and a_5 on BS$_2$ and a_4 and a_6 on BS$_3$ the final four output modes b_i ($i = 1, 2, 3, 4$) were produced. It has been theoretically demonstrated in Ref. [8] [see Eqs. (4) of Ref. [8]] that the four modes b_i are in the cluster state if the interfering phase difference of a_1 and a_5 is 0 and that of a_4 and a_6 is $\pi/2$; however, they are in the quadripartite GHZ state if both phase differences are controlled at 0. The calculated correlation variances of quadrature components of modes b_i for cluster and GHZ state are respectively

$$\langle \Delta^2(Y_{b1}^C - Y_{b2}^C) \rangle = \langle \Delta^2(X_{b3}^C - X_{b4}^C) \rangle = \frac{1}{2}e^{-2r},$$

$$\langle \Delta^2(X_{b1}^C + X_{b2}^C + g_3^C X_{b3}^C) \rangle = \frac{(g_3^C)^2 - 4g_3^C + 4}{16}e^{2r} + \frac{3(g_3^C)^2 + 4g_3^C + 4}{16}e^{-2r},$$

$$\langle \Delta^2(-g_2^C Y_{b2}^C + Y_{b3}^C + Y_{b4}^C) \rangle = \frac{(g_2^C)^2 - 4g_2^C + 4}{16}e^{2r} + \frac{3(g_2^C)^2 + 4g_2^C + 4}{16}e^{-2r}, \tag{2}$$

$$\langle \Delta^2(g_1^C X_{b1}^C + X_{b2}^C + 2X_{b3}^C) \rangle = \frac{3(g_1^C)^2 - 6g_1^C + 3}{16}e^{2r} + \frac{(g_1^C)^2 + 6g_1^C + 17}{16}e^{-2r},$$

$$\langle \Delta^2(-2Y_{b2}^C + Y_{b3}^C + g_4^C Y_{b4}^C) \rangle = \frac{3(g_4^C)^2 - 6g_4^C + 3}{16}e^{2r} + \frac{(g_4^C)^2 + 6g_4^C + 17}{16}e^{-2r},$$

and

$$\langle \Delta^2(X_{b1}^G + X_{b2}^G + g_3^G X_{b3}^G + g_4^G X_{b4}^G) \rangle = \frac{(2 - g_3^G - g_4^G)^2 + 2(g_3^G - g_4^G)^2}{16}e^{2r} + \frac{(2 + g_3^G + g_4^G)^2}{16}e^{-2r},$$

$$\langle \Delta^2(g_1^G X_{b1}^G + X_{b2}^G + X_{b3}^G + g_4^G X_{b4}^G) \rangle = \frac{(2 - g_1^G - g_4^G)^2 + 2(g_1^G - g_4^G)^2}{16}e^{2r} + \frac{(2 + g_1^G + g_4^G)^2}{16}e^{-2r},$$

$$\langle \Delta^2(g_1^G X_{b1}^G + g_2^G X_{b2}^G + X_{b3}^G + X_{b4}^G) \rangle = \frac{(2 - g_1^G - g_2^G)^2 + 2(g_1^G - g_2^G)^2}{16}e^{2r} + \frac{(2 + g_1^G + g_2^G)^2}{16}e^{-2r}, \tag{3}$$

$$\langle \Delta^2(Y_{b1}^G - Y_{b2}^G) \rangle = \langle \Delta^2(Y_{b2}^G - Y_{b3}^G) \rangle = \langle \Delta^2(Y_{b3}^G - Y_{b4}^G) \rangle = \frac{1}{2}e^{-2r}.$$

The superscript C and G designate the cluster and GHZ state, respectively. g_i^C and g_i^G are the gain factor (arbitrary real parameter). In experiments we may adjust the electronic gains of photocurrents to optimize the correlation variances. Calculating the minimum values of the expressions in Eqs. (2) and (3) we got the optimized gain factors

$$g_{\text{opt1}}^C = g_{\text{opt4}}^C = \frac{3e^{4r} - 3}{3e^{4r} + 1}, \qquad (4)$$

$$g_{\text{opt2}}^C = g_{\text{opt3}}^C = \frac{2e^{4r} - 2}{e^{4r} + 3}, \qquad (5)$$

for cluster state and

$$g_{\text{opt}}^G = g_{\text{opt1}}^G = g_{\text{opt2}}^G = g_{\text{opt3}}^G = g_{\text{opt4}}^G = \frac{e^{4r} - 1}{e^{4r} + 1}, \qquad (6)$$

for GHZ state, respectively.

The four modes b_i and the four local oscillation beams at 1080 nm deriving from the pump laser (not shown in Fig. 1) are sent to the four sets of the balanced-homodyne detectors (BHD$_{1-4}$), respectively, for measuring the fluctuation variances of the amplitude or phase quadratures of mode b_i. The measured photocurrent variances of each mode are combined by the positive (+) or negative (−) power combiner according to the different requirements of the correlation variances in Eqs. (2) and (3), then are sent to a spectrum analyzer (SA) for recording the desired variety correlation variances.

The experimentally measured squeezing degrees of the output fields from NOPA1 and NOPA2 equal to 3.5 ± 0.1 dB below the SNL (the corresponding squeezing parameter r equals to 0.40 ± 0.01). During the measurements the pump power of NOPAs at 540 nm wavelength is ~ 200 mW below the oscillation threshold of 255 mW and the intensity of the injected signal at 1080 nm is 10 mW.

Adjusting the electronic gains to the optimal values the measured correlation variances of $\langle \Delta^2(Y_{b1}^C - Y_{b2}^C) \rangle$, $\langle \Delta^2(X_{b1}^C + X_{b2}^C + g_{\text{opt2}}^C X_{b3}^C) \rangle$, $\langle \Delta^2(X_{b3}^C - X_{b4}^C) \rangle$, $\langle \Delta^2(-g_{\text{opt2}}^C Y_{b2}^C + Y_{b3}^C + Y_{b4}^C) \rangle$, $\langle \Delta^2(g_{\text{opt1}}^C X_{b1}^C + X_{b2}^C + 2X_{b3}^C) \rangle$, and $\langle \Delta^2(-2Y_{b2}^C + Y_{b3}^C + g_{\text{opt1}}^C Y_{b4}^C) \rangle$ for the cluster state are 1.3 ± 0.1 dB, 1.1 ± 0.1 dB, 1.2 ± 0.1 dB, 1.0 ± 0.1 dB, 1.2 ± 0.1 dB, and 1.2 ± 0.1 dB below the SNL, respectively, which are shown in Fig. 2. The measured correlation variances of $\langle \Delta^2(Y_{b1}^G - Y_{b2}^G) \rangle$, $\langle \Delta^2(X_{b1}^G + X_{b2}^G + g_{\text{opt}}^G X_{b3}^G + g_{\text{opt}}^G X_{b4}^G) \rangle$, $\langle \Delta^2(Y_{b2}^G - Y_{b3}^G) \rangle$, $\langle \Delta^2(g_{\text{opt}}^G X_{b1}^G + X_{b2}^G + X_{b3}^G + g_{\text{opt}}^G X_{b4}^G) \rangle$, $\langle \Delta^2(Y_{b3}^G - Y_{b4}^G) \rangle$, and $\langle \Delta^2(g_{\text{opt}}^G X_{b1}^G + g_{\text{opt}}^G X_{b2}^G + X_{b3}^G + X_{b4}^G) \rangle$ for the GHZ state are 1.2 ± 0.1 dB, 1.2 ± 0.1 dB, 1.2 ± 0.1 dB, 1.1 ± 0.1 dB, 1.3 ± 0.1 dB, and 1.1 ± 0.1 dB below the SNL, respectively (see Fig. 3). The optimal gains used in the measurements are $g_{\text{opt1}}^C = 0.267$, $g_{\text{opt2}}^C = 0.578$, and $g_{\text{opt}}^G = 0.446$.
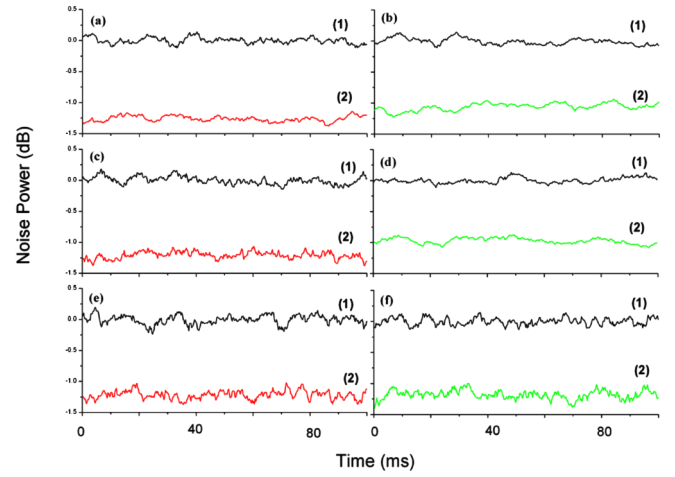

FIG. 2 (color online). The measured correlation variances of the cluster state at 2 MHz. (a) $\langle \Delta^2(Y_{b1}^C - Y_{b2}^C) \rangle$; (b) $\langle \Delta^2(X_{b1}^C + X_{b2}^C + g_{\text{opt2}}^C X_{b3}^C) \rangle$; (c) $\langle \Delta^2(X_{b3}^C - X_{b4}^C) \rangle$; (d) $\langle \Delta^2(-g_{\text{opt2}}^C Y_{b2}^C + Y_{b3}^C + Y_{b4}^C) \rangle$; (e) $\langle \Delta^2(g_{\text{opt1}}^C X_{b1}^C + X_{b2}^C + 2X_{b3}^C) \rangle$; (f) $\langle \Delta^2(-2Y_{b2}^C + Y_{b3}^C + g_{\text{opt1}}^C Y_{b4}^C) \rangle$. (1) The corresponding shot noise limit. (2) The correlation noise power. The measurement parameters of SA: RBW (resolution bandwidth)-30 kHz; VBW (video bandwidth)-30 Hz.

Based on the same method of concluding the full inseparability criteria of multipartite CV GHZ entanglement in Ref. [12] we derived the sufficient requirements of full inseparability for the quadripartite cluster state. When the following three inequalities are satisfied simultaneously the four submodes b_i are in a fully inseparable cluster entangled state:
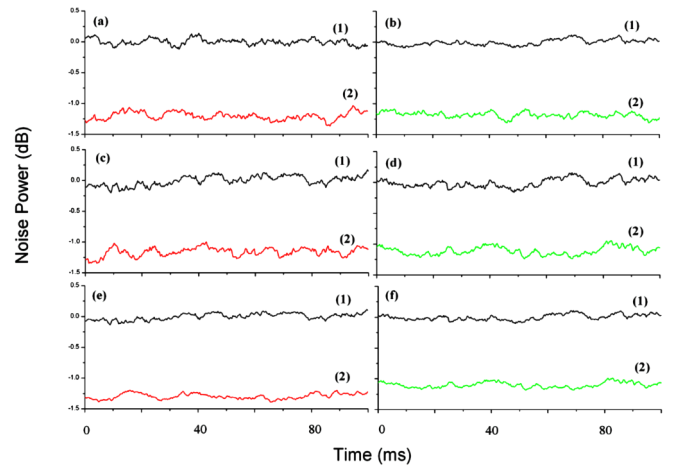

FIG. 3 (color online). The measured correlation variances of the GHZ state at 2 MHz. (a) $\langle \Delta^2(Y_{b1}^G - Y_{b2}^G) \rangle$; (b) $\langle \Delta^2(X_{b1}^G + X_{b2}^G + g_{\text{opt}}^G X_{b3}^G + g_{\text{opt}}^G X_{b4}^G) \rangle$; (c) $\langle \Delta^2(Y_{b2}^G - Y_{b3}^G) \rangle$; (d) $\langle \Delta^2(g_{\text{opt}}^G X_{b1}^G + X_{b2}^G + X_{b3}^G + g_{\text{opt}}^G X_{b4}^G) \rangle$; (e) $\langle \Delta^2(Y_{b3}^G - Y_{b4}^G) \rangle$; (f) $\langle \Delta^2(g_{\text{opt}}^G X_{b1}^G + g_{\text{opt}}^G X_{b2}^G + X_{b3}^G + X_{b4}^G) \rangle$. (1) The corresponding shot noise limit. (2) The correlation noise power. The measurement parameters of SA are same as Fig. 2.

$$\text{I}^C \langle \Delta^2 (Y_{b1}^C - Y_{b2}^C) \rangle + \langle \Delta^2 (X_{b1}^C + X_{b2}^C + g_{\text{opt2}}^C X_{b3}^C) \rangle < 1,$$

$$\text{II}^C \langle \Delta^2 (X_{b3}^C - X_{b4}^C) \rangle + \langle \Delta^2 (-g_{\text{opt2}}^C Y_{b2}^C + Y_{b3}^C + Y_{b4}^C) \rangle < 1,$$

$$\text{III}^C \langle \Delta^2 (g_{\text{opt1}}^C X_{b1}^C + X_{b2}^C + 2X_{b3}^C) \rangle$$

$$+ \langle \Delta^2 (-2Y_{b2}^C + Y_{b3}^C + g_{\text{opt1}}^C Y_{b4}^C) \rangle < 2. \qquad (7)$$

Substituting the measured correlation variances into the left sides of I^C, II^C, and III^C in Eq. (7) we have $\text{I}^C = 0.83 \pm 0.01$, $\text{II}^C = 0.85 \pm 0.02$, and $\text{III}^C = 1.94 \pm 0.02$; all of them are smaller than the normalized SNL. It means the obtained modes are in a fully inseparable cluster entangled state.

From Ref. [12] we can directly write out the criteria of the full inseparability for quadripartite GHZ state:

$$\text{I}^G \langle \Delta^2 (Y_{b1}^G - Y_{b2}^G) \rangle$$

$$+ \langle \Delta^2 (X_{b1}^G + X_{b2}^G + g_{\text{opt}}^G X_{b3}^G + g_{\text{opt}}^G X_{b4}^G) \rangle < 1,$$

$$\text{II}^G \langle \Delta^2 (Y_{b2}^G - Y_{b3}^G) \rangle$$

$$+ \langle \Delta^2 (g_{\text{opt}}^G X_{b1}^G + X_{b2}^G + X_{b3}^G + g_{\text{opt}}^G X_{b4}^G) \rangle < 1, \qquad (8)$$

$$\text{III}^G \langle \Delta^2 (Y_{b3}^G - Y_{b4}^G) \rangle$$

$$+ \langle \Delta^2 (g_{\text{opt}}^G X_{b1}^G + g_{\text{opt}}^G X_{b2}^G + X_{b3}^G + X_{b4}^G) \rangle < 1.$$

Similarly we get $\text{I}^G = 0.84 \pm 0.02$, $\text{II}^G = 0.85 \pm 0.01$, and $\text{III}^G = 0.84 \pm 0.02$ from the experimental results. It shows that all three inequalities in Eq. (8) are satisfied and thus the quadripartite GHZ entanglement of the four optical modes are demonstrated experimentally.

For achieving the measurements of a variety of the correlation variances under same experimental conditions the pump laser has to operate stably in the whole experimental process. The resonating frequencies of the laser and the two NOPAs must be locked in a longer term. In addition, 9 sets of the phase-locking system are, respectively, used for locking the relative phases between the pump laser and the injected signal beam of the two NOPAs to π, the phase difference between b_i and local oscillation beam in the four sets of BHD_i to 0 (for amplitude measurement) or $\pi/2$ (for phase measurement), and the interference phases between two combined beams on BS_1, BS_2, and BS_3 to 0 or $\pi/2$ according to the different requirements for generating cluster or GHZ state mentioned above. The standard sideband frequency locking [18] and the interference feedback [19] technologies are utilized in the frequency and the relative phase locking, respectively.

For conclusion, we have experimentally produced the CV quadripartite cluster and GHZ entangled states for the first time to the best of our knowledge. In this experiment we definitely identified and applied both amplitude and phase squeezed states produced from a NOPA simultaneously, which provides a new scheme to obtain two CV quadrature squeezed states from an implement. The investigation has demonstrated the possibility to generate and manipulate two types of CV quadripartite entanglement using two-mode squeezed states and linear optics, which is the necessary base for realizing quantum computation and more complicated quantum communication network.

*Electronic address: jiaxj@sxu.edu.cn

[1] J. Jing *et al.*, Phys. Rev. Lett. **90**, 167903 (2003)

[2] H. Yonezawa, T. Aoki, and A. Furusawa, Nature (London) **431**, 430 (2004); T. Aoki *et al.*, Phys. Rev. Lett. **91**, 080404 (2003).

[3] A. M. Lance *et al.*, Phys. Rev. Lett. **92**, 177903 (2004).

[4] P. van Loock and S. L. Braunstein, Phys. Rev. Lett. **84**, 3482 (2000).

[5] A. Ferraro and M. G. A. Paris, Phys. Rev. A **72**, 032312 (2005).

[6] J. Zhang, C. Xie, and K. Peng, Phys. Rev. Lett. **95**, 170501 (2005).

[7] J. Zhang, C. Xie, and K. Peng, Phys. Rev. A **73**, 042315 (2006).

[8] J. Zhang and S. L. Braunstein, Phys. Rev. A **73**, 032318 (2006).

[9] N. C. Menicucci *et al.*, Phys. Rev. Lett. **97**, 110501 (2006).

[10] Z. Zhao *et al.*, Nature (London) **430**, 54 (2004).

[11] P. Walther *et al.*, Nature (London) **434**, 169 (2005).

[12] P. van Loock and A. Furusawa, Phys. Rev. A **67**, 052315 (2003).

[13] Z. Y. Ou, S. F. Pereira, and H. J. Kimble, Appl. Phys. B **55**, 265 (1992).

[14] Y. Zhang, H. Su, C. Xie, and K. Peng, Phys. Lett. A **259**, 171 (1999).

[15] Y. Zhang *et al.*, Phys. Rev. A **62**, 023813 (2000).

[16] X. Li *et al.*, Phys. Rev. Lett. **88**, 047904 (2002).

[17] P. D. Drummond and M. D. Reid, Phys. Rev. A **41**, 3930 (1990).

[18] P. W. Drever *et al.*, Appl. Phys. B **31**, 97 (1983).

[19] T. Zhang *et al.*, Phys. Rev. A **67**, 033802 (2003).